

# Two-dimensional spectroscopy of double-barred galaxies

A.V. Moiseev

Special Astrophysical Observatory RAS, Nizhniĭ Arkhyz, Karachai-Cherkessia, 357147 Russia

Received May 29, 2002

**Abstract.** We describe the results of our spectroscopy for a sample of barred galaxies whose inner regions exhibit an isophotal twist commonly called a secondary bar. The line-of-sight velocity fields of the ionized gas and stars and the light-of-sight velocity dispersion fields of the stars were constructed from two-dimensional spectroscopy with the 6m Special Astrophysical Observatory telescope. We detected various types of non-circular motions of ionized gas: radial flows within large-scale bars, counter-rotation of the gas and stars at the center of NGC 3945, a polar gaseous disk in NGC 5850, etc. Our analysis of the optical and near-infrared images (both ground-based and those from the Hubble Space Telescope) revealed circumnuclear minispirals in five objects. The presence of an inner (secondary) bar in the galaxy images is shown to have no effect on the circumnuclear kinematics of the gas and stars. Thus, contrary to popular belief, the secondary bar is not a dynamically decoupled galactic structure. We conclude that the so-called double-barred galaxies are not a separate type of galaxies but are a combination of objects with distinctly different morphology of their circumnuclear regions. (c) 2002 MAIK Nauka/Interperiodica.

## 1. Introduction

According to observational estimates, galaxies with central bars account for a major fraction (50-70%) of the total number of nearby disk galaxies (Selwood and Wilkinson, 1993; Knapen et al., 2000b). The motion of stars and gaseous clouds within the bar differs markedly from unperturbed circular rotation; the radial flows of gas toward the center prove to be significant, as confirmed by direct observations (Afanasiev and Shapovalova, 1981; Duval and Monnet, 1985; Knappen et al., 2000a) and by numerous model calculations [see Lindblad (1999) for a review]. The central regions of such galaxies are decoupled in their dynamical parameters, star-formation rates, and densities of the gas and dust. For example, the molecular-gas density within the central kiloparsec in barred galaxies is an order of magnitude higher than that in unbarred galaxies (Sakamoto et al. 1999).

The dynamical effect of the bar is considered to be a major mechanism of transporting interstellar gas from the disk into the circumnuclear region, where it becomes fuel for a circumnuclear starburst or an active nucleus (Combes, 2001). In the latter case, however, the relationship between the bar and the active (for a disk galaxy, Seyfert) nucleus is far from being unequivocal. Thus, the relative fraction of bars in Seyfert galaxies only slightly exceeds this fraction in galaxies without active nuclei (Knapen et al., 2000). The main problem is that the gas in the bar is concentrated not in the nucleus itself but in

a ring of several hundred parsecs in radius, in the region of the inner Lindblad resonance. Therefore, an additional mechanism is required to take angular momentum away from the gas at a distance of 100 – 1000 pc from the centre and to transport the gas into the region where the gravitational forces of a central supermassive black hole are in action (Combes, 2001). An elegant solution to the problem of mass transport to an active nucleus is the assumption made by Shlosman et al. (1989) that another bar can be formed in the gaseous disk (ring) within a large-scale bar that again produces flows of gas toward the nucleus. The system of two bars is capable of sweeping away the interstellar medium on scales of several kpc and of concentrating it at distances of 1 – 10 pc from the centre. Recently, this process was numerically simulated by Heller et al. (2001), although, in essence, the authors considered the evolution of the inner elliptical ring rather than the stellar-gaseous bar.

Increased interest in double bars stems from the fact that something like that is occasionally seen in the images of barred galaxies. Vaucouleurs (1975) detected a bar-like structure within the large-scale bar in NGC 1291. The first systematic observational study of a double-barred galaxy was undertaken by Buta and Crocker (1993). They published a list of 13 galaxies with an arbitrary orientation of the inner (secondary) bar relative to the outer (primary) bar. Analysis of the isophotes shapes revealed secondary bars in the optical (Wozniak et al., 1995; Erwin and Sparke 1999) and NIR images of galaxies (Friedli et al., 1996; Jungwiert et al., 1997; Laine et al., 2002). An extensive

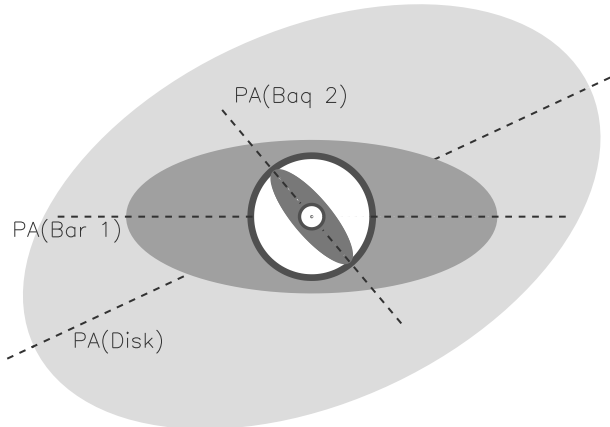


**Fig. 1.** A schematic view of a double-barred galaxy in projection onto the plane of the sky. The ring that corresponds to the region of the inner Lindblad resonance in the outer bar is highlighted. The principal isophotal orientations (see Subsect. 3.1) are indicated by dashed lines.

bibliography and a list of 71 candidates for double bars compiled from literature are given in Moiseev (2001b).

Although there are now many papers on this subject, the dynamical behavior of such stellar configurations is still unclear. Maciejewski and Sparke (2000) showed that closed orbital loops maintaining the shapes of both bars that rotate with different angular velocities could exist. Similar independently rotating structures also occasionally appear in experiments on simulating stellar-gaseous disks (Pfenninger and Norman, 1990; Friedli and Martinet, 1993). The behavior of the gas in double bars was numerically analyzed by Maciejewski et al., (2002) and Shlosman and Heller (2002). Figure 1 shows a scheme of a galaxy with two independently rotating bars, which may actually be considered to be universally accepted.

It should be noted that, despite several interesting results obtained in numerical experiments, they are strongly model-dependent. Khoperskov et al., (2001) showed that a secondary bar could periodically arise only at certain stages of the galaxy dynamical evolution; a long-lived secondary bar cannot yet be simulated (Friedli and Martinet, 1993; Erwin and Sparke, 2002). New observational data are required to verify contradictory theoretical predictions.

Numerous observational studies indicate that in the case of double bars, we probably come across a new structural feature of barred galaxies. However, the vast majority of these studies are based only on photometric data, when an extended structure is seen in the image of the galaxy within its primary bar (Fig. 2). Formal application of an isophotal analysis (Wozniak et al., 1995) even allowed several authors to distinguish triple bars (Jungwiert et al., 1997; Friedli et al., 1996; Erwin and Sparke, 1999) without any reasoning on the dynamical stability of such configurations. However, the observed photometric structural features of such galaxies can also be explained in less exotic ways, without invoking secondary or third bars. An oblate bulge, an intricate distribution of star-forming re-

gions and dust in the circumnuclear region, and an elliptical ring in the resonance region of the major bar can all create the illusion of a secondary bar in the galaxy images (Friedli et al., 1996; Moiseev, 2001b). Kinematic data, i.e., measurements of the line-of-sight velocities and velocity dispersions of the gas and stars, are required to solve the problem. Since the observed objects are definitely not axisymmetric, two-dimensional spectroscopy can be of great help. It allows the two-dimensional distributions of line-of-sight velocities and their dispersions in the plane of the sky to be constructed.

In this paper, we discuss the results of the first systematic study of such galaxies by using two-dimensional spectroscopy carried out in 2000-2002 with the goal to answer the following question: Are the secondary bars dynamically decoupled systems? Since the observational data themselves were described in detail by Moiseev et al. (2002), we discuss here only the most important features of the objects under study. The observing techniques are described in Sect. 2. In Sect. 3, we analyze the velocity and velocity dispersion distributions in the galaxies and describe the minispiral structures detected in the central regions of several galaxies. Our results are discussed in Sect. 4 and our main conclusion is formulated in Sect. 5.

## 2. Observations and data reduction

We drew our sample from the list of candidates for double bars (Moiseev, 2001b) based on convenience of their observation with the 6m telescope:  $\delta > 0$ ; the diameter of the secondary bar fits into the MPFS field of view. Observational data were obtained for 13 galaxies, which account for about half of the total number of such objects in the northern sky. The Table 1 gives the name of the galaxy, its morphological type from the NED database, and the sizes of the apparent semi-major axes of the outer ( $a_1$ ) and inner ( $a_2$ ) bars in arcseconds with a reference to the corresponding papers.

All spectroscopic and some of the photometric observations were carried out with the 6m Special Astrophysical Observatory (SAO, Russia) telescope at 1 – 2.5'' seeing. The detector was a TK1024 CCD array. A log of observations and a detailed description of individual galaxies and the data reduction procedure were given by Moiseev et al. (2002).

The circumnuclear regions of all galaxies were observed with the Multipupil Field Spectrograph (MPFS) (Afanasyev et al., 2001). It simultaneously takes spectra from 240 spatial elements in the shape of square lenses that comprise a  $16 \times 15$  matrix in the plane of the sky. The angular size of a single matrix element is 1''. The MPFS spectrograph is described in the Internet at [http://www.sao.ru/~gafan/devices/mpfs/mpfs\\_main.htm](http://www.sao.ru/~gafan/devices/mpfs/mpfs_main.htm). The observations were carried out in the spectral range  $\lambda 4800 - 6100\text{\AA}$  and, for several galaxies, in the range  $\lambda 5800 - 7100\text{\AA}$ ; the dispersion was  $1.35\text{\AA}$  per pixel. The covered spectral range included absorption features typical of the old (G-K-type) galactic stellar population.

**Table 1.** Parameters of the observed galaxies

Name	Type	$a_1$ (")	$a_2$ (")	References to photometry
NGC 470	SAb	32	8	Wozniak et al. (1995); Friedli et al. (1996)
NGC 2273	SBa	24	8	Mulchaey et al. (1997)
NGC 2681	SAB0/a	29	5	Wozniak et al. (1995); Erwin and Sparke (1999)
NGC 2950	SB0	38	6	Wozniak et al. (1995); Friedli et al. (1996)
NGC 3368	SABab	24	4	Jungwiert et al. (1997)
NGC 3786	SABa	25	7	Afanasiev et al. (1998)
NGC 3945	SB0	42	20	Wozniak et al. (1995); Erwin and Sparke (1999)
NGC 4736	SAab	26	10	Shaw et al. (1993)
NGC 5566	SBab	24	6	Jungwiert et al. (1997)
NGC 5850	SBb	84	9	Buta and Crocker (1993); Wozniak et al. (1995)
NGC 5905	SBb	37	6	Wozniak et al. (1995); Friedli et al. (1996)
NGC 6951	SABbc	44	5	Wozniak et al. (1995)
NGC 7743	SB0	57	10	Wozniak et al. (1995)

The line-of-sight velocity and velocity dispersion fields of the stars were constructed by using a cross-correlation technique modified for work with MPFS data (Moiseev, 2001a). The line-of-sight velocities and velocity dispersions were determined with an accuracy of  $\sim 10 \text{ km s}^{-1}$ . Based on the MPFS observations, we also mapped the two-dimensional intensity distribution and the velocity field of the ionized gas in the  $H_\beta$ ,  $[\text{O III}]\lambda 4959, 5007 \text{ \AA}$  and  $[\text{N II}]\lambda 6548, 6583 \text{ \AA}$  emission lines. The line-of-sight velocities were measured with an accuracy of  $\sim 10 \text{ km s}^{-1}$ . No emission features were detected in NGC 2950 and NGC 5566. Six galaxies with intense emission features were observed with a scanning interferometer Fabry-Perot (IFP) in the 235th order of interference in a spectral region near the wavelength of the  $H_\alpha$  line. The instrumental profile width was  $2.5 \text{ \AA}$  ( $\sim 110 \text{ km s}^{-1}$ ); the field of view was about  $5'$  with a scale of  $0.56 - 0.68''$  per pixel. The instrument and reduction techniques were described previously (Moiseev, 2002). We constructed the velocity fields of the ionized gas in  $H_\alpha$  or  $[\text{N II}]\lambda 6583 \text{ \AA}$  with an accuracy of  $\sim 5 \text{ km s}^{-1}$ .

The optical V- and R-band images of seven galaxies were obtained at the prime focus of the 6m telescope using the SCORPIO focal reducer (its description can be found in the Internet at <http://www.sao.ru/~moisav/scorpio/scorpio.html>). The field of view is  $4.8'$  with a scale of  $0.28''$  per pixel. In addition, we used the JHK-band images obtained with the 2.1m OAN telescope in Mexico [for more detail, see Moiseev et al., (2002)]. We also used the galaxy images from the Hubble Space Telescope (HST) archive obtained with the Wide-Field and Planetary Camera (WFPC2) and with the Near-IR Camera (NICMOS). As an example of the observational data used, Fig. 2 shows the images of NGC 2273 and NGC 2950 and Fig. 3 shows the velocity fields of the gas and

### 3. Analysis of the spectroscopic and photometric observations

#### 3.1. Velocity dispersion

The velocity dispersion distribution of the stellar disk is one of its important parameters. It allows unambiguous multicomponent models of the mass distribution in galaxies to be constructed (Khoperskov et al., 2002). Numerical calculations show that because of the bar formation, the velocity dispersion distribution in the galactic disk differs greatly from the unperturbed (without a bar and spiral structure) axisymmetric case (Miller and Smith, 1979; Vauterin and Dejonghe, 1997). The bar is a much hotter dynamical subsystem; the velocity dispersion in it increases sharply. In addition, the velocity ellipsoid is found to be highly anisotropic. This anisotropy manifests itself in different distributions of the radial, azimuthal, and vertical velocity dispersions in the disk plane. The model maps of the line-of-sight stellar velocity dispersion constructed for various disk and bar orientations (Miller and Smith, 1979; Vauterin and Dejonghe, 1997; Khoperskov et al., 2001) indicate that the line-of-sight velocity dispersion ( $\sigma_*$ ) distribution within the bar is symmetric about the bar major axis rather than about the disk major axis (line of nodes), as would be the case in the absence of a bar. Unfortunately, the observational manifestations of the velocity-dispersion anisotropy in the  $\sigma_*$  distribution are few in number. The series of papers by Kormendy (1982, 1983) are an example of the most consistent approach to measuring the velocity-dispersion anisotropy in barred galaxies. However, most authors restrict themselves to measuring  $\sigma_*$  along one or two spectrograph slit directions. The two-dimensional  $\sigma_*$  maps used here are much more informative. Figures 3c and 3d show the isolines of the  $\sigma_*$  distribution that form ellipsoidal, elongated structures asymmetric about the disk line of nodes in the central regions of NGC 2273 and NGC 2950.

To quantitatively describe the deviation of the  $\sigma_*$  distribution from the axisymmetric case, we used the

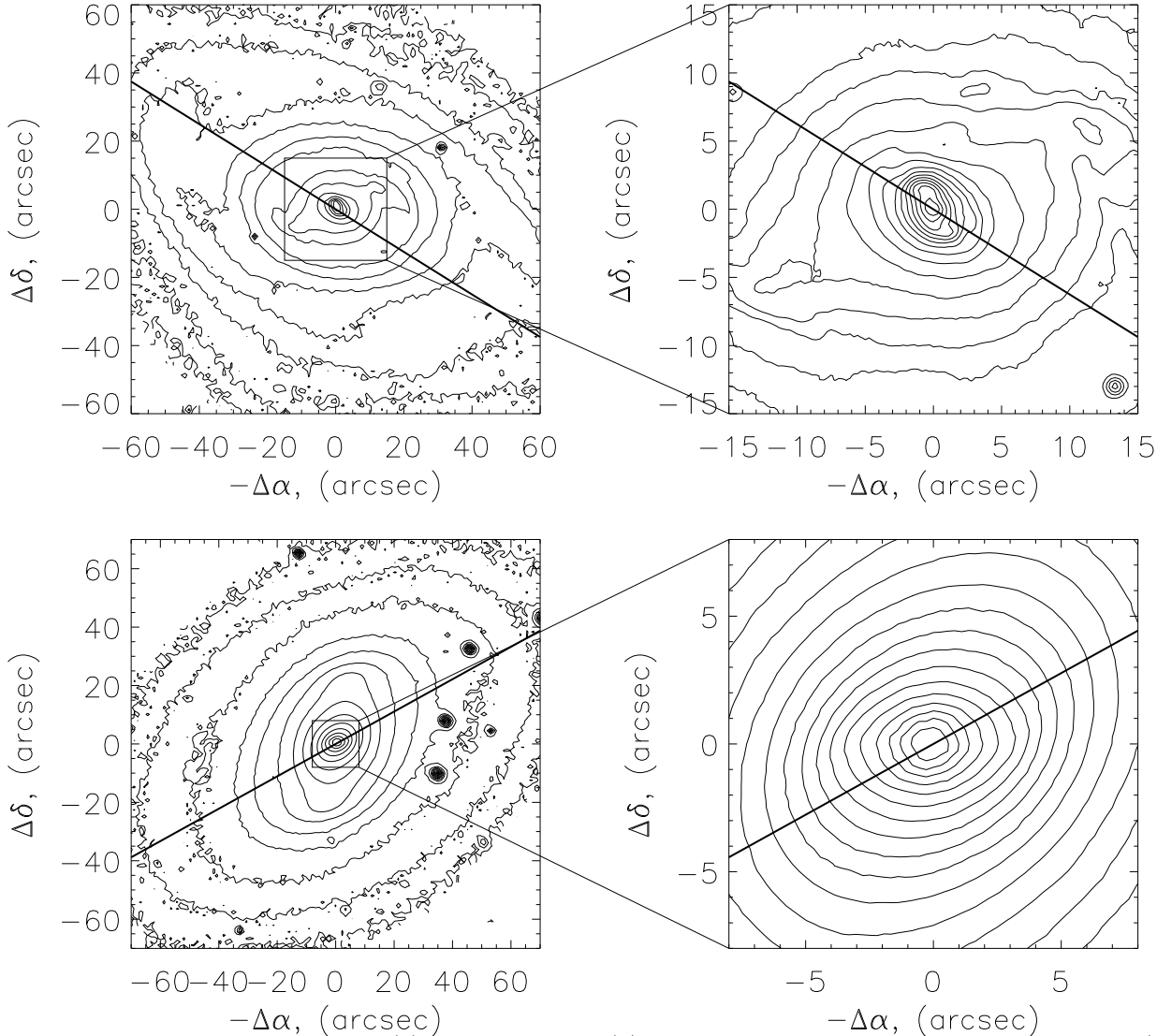


**Fig. 2.** The R-band images of (a) NGC 2273 and (b) NGC 2950 obtained with the 6m telescope; (c) and (d) the enlarged central regions highlighted by the square in panels (a) and (b), respectively. The inner isophotal twist relative to the outer bars is clearly seen. The heavy lines indicate the orientation of the line of nodes of the disk. stars and the velocity dispersion fields of the stars in NGC 2273, NGC 2950, and NGC 3945.

Fourier expansion of the observed velocity dispersion field in terms of position angle  $PA$ :

$$\sigma_*(r, PA) = A_0(r) + \sum_{m=1}^N A_m(r) \cos(m PA + \phi_m(r)), \quad (1)$$

where  $r$  is the distance from the center in the plane of the sky;  $A_m$  and  $\phi_m$  are the amplitude and phase of the harmonic with number  $m$ , respectively; and  $N = 6 - 8$  is the maximum number of harmonics. Our technique is similar to that used by Lyakhovich et al. (1997) to analyze the velocity fields but differs from it in that the Fourier expansion is made in terms of  $PA$  rather than in terms of the azimuthal angle in the galactic plane. In addition, it was shown in the above paper and in subsequent papers (see, e.g., Fridman et al., 2001) that for the velocity field of the gaseous disk in a spiral galaxy, the principal expan-

sion harmonics are related to the spatial velocity vector components. For analysis of the  $\sigma_*$  fields, we cannot yet offer such a clear physical interpretation of the Fourier spectrum, because the combined contribution of the bulge and the disk with the bar is observed in the central regions under study. However, since our simulations indicate that the  $\sigma_*$  isolines in the bar form an ellipsoidal structure, this must correspond to a situation where the  $m = 2$  harmonic and, possibly, the succeeding even harmonics have a maximum amplitude in (1). The direction of the major axis of this structure corresponds to the line of maximum of the second harmonic:  $PA_2 = -\phi_2/2 \pm 180^\circ$ .

We broke down the velocity dispersion fields into rings with the center coincident with the photometric center of the continuum image. To provide a sufficient number of points in relation (1), each image element was broken down into four  $0.5 \times 0.5''$  elements. Experiments with anal-

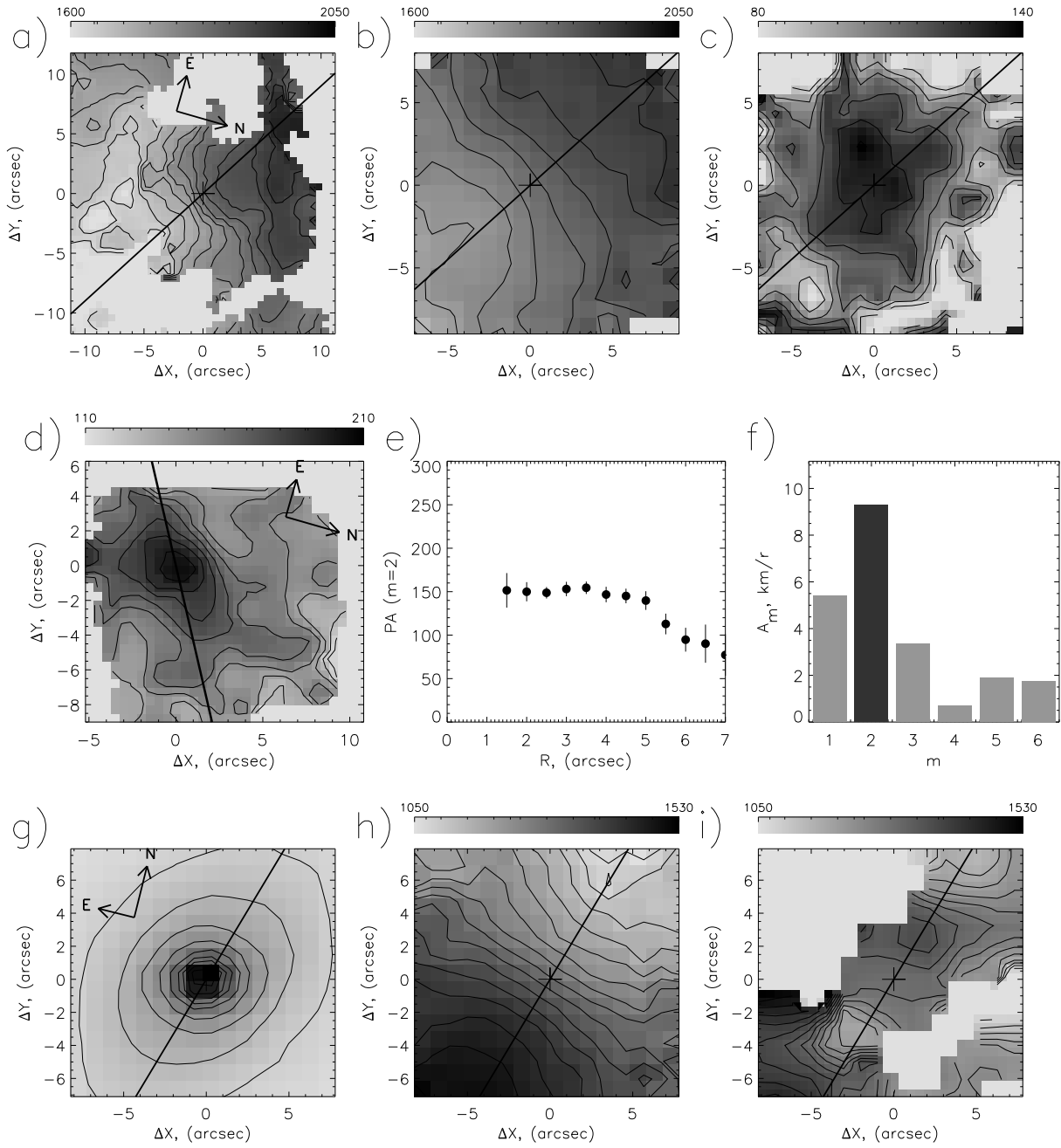


**Fig. 3.** Results of the observations of three galaxies. The gray scale is velocity in  $\text{km s}^{-1}$  and the heavy line indicates the orientation of the line of nodes everywhere. NGC 2273: (a) the gas velocity field constructed from IFP observations; (b), (c) the stellar velocity and velocity dispersion fields. NGC 2950: (d) the velocity dispersion field; (e) the radial dependence of the position angle of the maximum of the second harmonic in the Fourier spectrum  $\sigma_*$ ; (f) the mean harmonic amplitude in the Fourier spectrum  $\sigma_*$ . NGC 3945: (g) the continuum MPFS image of the center; (h) the stellar velocity field; (i) the velocity field of the gas with counter-rotation in the central region.

ysis of various images show that this procedure introduces no significant distortions into the spectrum of the first harmonics, at least for  $m < 4 - 5$ . The position angle of the symmetry axis in the velocity dispersion distribution is defined as the mean value of the  $r$  dependence of  $PA_2$ , provided that there is a segment with an approximately constant  $PA_2$  and that the second harmonic dominates in the Fourier spectrum at given  $r$ . For NGC 2950, this radii range is  $r = 1 - 5''$  (Figs. 3e, 3f). The succeeding

change in  $PA_2$  at large distances stems from the fact that the galaxy does not lie exactly at the center of the MPFS field of view (Fig. 3d). Therefore, there are few pairs of diametrically opposite points in the velocity dispersion field for  $r > 5''$ , causing the spectrum of the even harmonics to be distorted.

The following three principal isophotal orientations can be distinguished in the image of a double-barred galaxy: the position angle of the disk,  $PA(\text{Disk})$ , and the

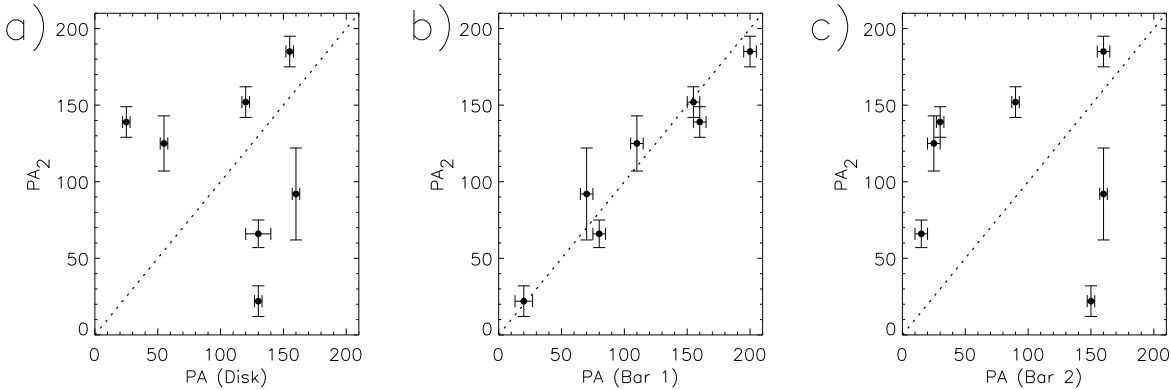


**Fig. 4.** Relation between the position angle of the second harmonic in the velocity dispersion distribution and the position angle of the disk (a) and the two bars (b) and (c). The dotted line represents a direct proportionality of PAs (not the best fit!)

position angles of the bars,  $PA(\text{Bar } 1)$  and  $PA(\text{Bar } 2)$ , shown in Fig. 1. According to the above considerations, if there are two dynamically independent bars, then each of these directions must be the symmetry axis in the apparent  $\sigma_*$  distribution on the corresponding distance scale. What actually determines the velocity dispersion distribution in the central region? To answer this question, we considered the relations between the position angle  $PA_2$  of the symmetry axis of the velocity dispersion field and these three directions shown in Fig. 4. This figure shows data only for those seven objects from our sample in which the second harmonic dominates in the Fourier spectrum of the azimuthal  $\sigma_*$  distribution at  $r = 1 - 6''$ . We see that in the galaxies under study, the direction  $PA_2$  in the circumnuclear region ( $r < 5 - 6''$ ) coincides (within the error limits) only with the orientation of the outer bar and correlates neither with the major axis of the inner bar (Fig. 4c) nor with the line of nodes of the disk (Fig. 4a).

Since the central regions in galaxies of mostly early morphological types were observed (see the Table 1), bulge stars must contribute significantly to the velocity dispersion. However, if the bulge is spherical, then it will affect only the amplitude of the  $m = 0$  harmonic, because the expansion (1) is made in terms of the angle in the plane of the sky. If the bulge is oblate but axisymmetric (spheroidal), then this will cause an increase in the amplitude of the second harmonic. The line of its maximum must coincide with the line of nodes of the disk, because the symmetry of the observed  $\sigma_*$  distribution is similar to the case of a disk with a different apparent axial ratio. However, Fig. 4a shows no correlation between  $PA_2$  and the line of nodes. If, alternatively, the bulge is triaxial, then it will produce an isophotal twist in the central region in projection onto the plane of the sky (Wozniak et al., 1995) and will be barely distinguishable from the inner bar. However, Fig. 4c shows no correlation between the symmetry direction of the velocity dispersion and the inner isophotal orientation.

Thus, the location of the line of maximum of the second harmonic in the Fourier expansion of the velocity dispersion field correlates only with the outer bar. This large-scale bar determines the dynamics of the stellar component even in those regions where the isophotal twist attributed to the secondary bar is observed.

### 3.2. Velocity fields

We determined the radial dependences of the position angle of the dynamical major axis (the line of maximum line-of-sight velocity gradient) from the velocity field by the method of inclined rings (Begeman, 1989). The velocity fields were broken down into elliptical rings about  $1''$  in width aligned with the outer galactic disk. In each ring, we determined the optimum dynamical position angle  $PA_{dyn}$  in the approximation of circular rotation [for more details, see Begeman, 1989; Moiseev and Mustsevoi, 2000].

The gaseous clouds move within the bar in such a way that the observed  $PA_{dyn}$  ceases to be aligned with the line of nodes of the disk (Chevalier and Furenlid, 1978); the dynamical axis turns in a sense opposite to the line of nodes compared with the position angle of the inner isophotes (Moiseev and Mustsevoi, 2000). In other words, the lines of equal line-of-sight velocities seek to elongate along the bar. A similar effect must also be observed in the stellar velocity field, as shown both by numerical simulations (Vauterin and Dejonghe, 1997) and by analytic calculations of the stellar dynamics in a triaxial gravitational potential (Monnet et al., 1992).

Figure 5 shows the radial dependences of the position angles of the dynamical axis and the major axis of the inner isophotes in several objects. We determined the isophotal orientation in NGC 2950 and NGC 3786 using the HST images obtained with the WFPC2 camera through a F814W filter and with the NICMOS 1 camera through a F160W filter, respectively. The R-band image of NGC 5850 was taken from the digital atlas by Frei et al.

(1996). In NGC 2950, the isophotal orientation changes by more than  $50^\circ$  (Fig. 5a), but  $PA_{dyn}$  for the stellar component is virtually aligned with the line of nodes. Neither the outer bar nor the inner bar have an appreciable effect on the stellar velocity field. This is probably because here, both stellar motions within the bar and the rotation of the bulge, whose contribution in this lenticular galaxy must be significant, are observed along the line-of-sight. Since the spectral resolution was too low to separate the two dynamical components in the line-of-sight velocity distribution (LOSVD), the mean velocity field corresponds to circular rotation. As was noted in Subsect. 3.1, the stellar component associated with the outer bar in NGC 2950 shows up in the distribution of the velocity dispersion, whose increase points to a broadening of the LOSVD in the bar region.

A similar pattern of stellar motion is observed in NGC 2273, NGC 3945, NGC 5566, NGC 5850, and NGC 5905. In four galaxies (NGC 470, NGC 2681, NGC 4736, and NGC 6951), there are significant ( $7-20^\circ$ ) deviations of  $PA_{dyn}$  for stars from the line of nodes of the outer disk; these deviations of the dynamical axis are not related to the orientation of the inner bar but are exactly in the opposite direction compared with the isophotes of the outer bar. Here, as with the velocity dispersion, the stellar motions are affected by the outer bar rather than the inner bar, as should be the case for the model of independently rotating bars described in Sect. 1.

In NGC 3786, on the scale of the inner bar ( $r < 6''$ ),  $PA_{dyn}$  deviates from the line of nodes by more than  $10^\circ$ ; the deviations are in the opposite direction compared with the central isophotes (Fig. 5b). Here, we actually observe a dynamically decoupled central minibar about  $\sim 2$  kpc in diameter. Its existence was first suspected by Afanasiev and Shapovalova (1981) when studying the gas kinematics in NGC 3786. In this galaxy, however, we cannot speak about a dynamically decoupled secondary bar, because a Fourier analysis of the surface-brightness distribution (Subsect. 3.3) indicates that the two-armed spiral mistaken by Afanasiev et al., (1998) for the outer bar is located in NGC 3786 at  $r = 7 - 20''$ .

The situation in NGC 3368 is similar. A dynamically decoupled inner bar is observed in this galaxy, but the outer bar described by Jungwiert et al., (1997) is actually part of the spiral structure. The paper that describes in detail the structure and dynamics of NGC 3368 is being prepared for publication (Sil'chenko et al., 2003).

The apparent kinematics of the ionized gas and stars in the objects under study are often different. Moreover, the ionized-gas velocities measured from permitted ( $H_\alpha$ ,  $H_\beta$ ) and forbidden ([O III], [N II]) lines can differ markedly. In NGC 3786, the dynamical axes in the stellar and gas velocity fields in  $H_\beta$  are aligned, while the position angles measured from the velocities in the [O III] line systematically deviate from them (Fig. 5b). A similar effect is also observed in NGC 470, NGC 2273, NGC 5905, and NGC 6951. These deviations may be due to the presence at the bar edges of shock fronts formed in the disk gas un-

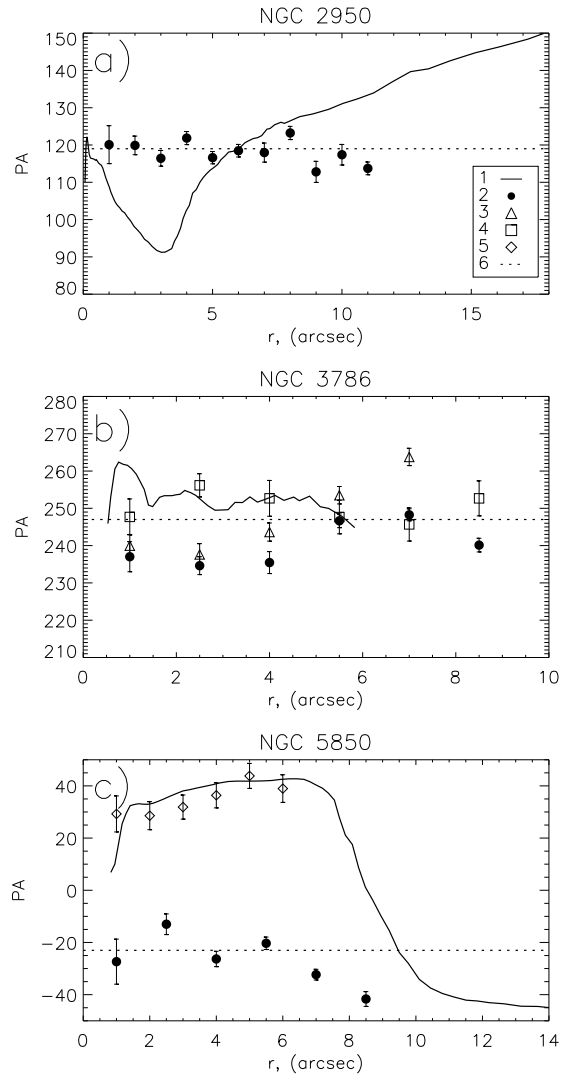


**Fig. 5.** The radial behavior of the position angle of the inner isophotes (1) and of the dynamical axis determined from stars (2) and from gas in the  $H_\beta$  (3), [O III] (4), and [N II] (5) lines for (a) NGC 2950, (b) NGC 3786, and (c) NGC 5850; 6, the line of nodes of the outer disk.

der action of the with the bar gravitational potential. The post-shock gas decelerates and emits in forbidden lines (Afanasiev and Shapovalova, 1981). The following alternative explanation is also possible: neglected stellar absorption features distort the  $H_\beta$  emission profile, which, in turn, introduces systematic errors into the gas line-of-sight velocity measurement. However, in galaxies with relatively intense emission features against the background of low-contrast absorption features, the velocity difference in forbidden and permitted lines in the bar region can be real.

In all the sample galaxies in which intense emission features were observed, the position angle  $PA_{dyn}$  measured from the gas is misaligned with the line of nodes of the outer disk, suggesting non-circular motions within the central kiloparsec. In five galaxies, the turn of the dynamical

ical axis is not related to the isophotal twist in the inner bar. At the same time, it is in the opposite direction relative to the isophotes of the outer bar. This implies that the outer bar determines the dynamics of the gas component, while the inner bar is not dynamically decoupled.

The non-circular gas motions in the remaining six galaxies are different in nature. Thus, in NGC 3368 and NGC 3786, they are associated with the central minibar and there is no outer bar here, as was mentioned above. In NGC 6951, the non-circular gas motions are associated with the central minispiral, which is discussed in the next section.

In NGC 470, the dynamical center, defined as the symmetry point of the velocity field, is displaced by  $4 - 5''$  ( $0.6 - 0.8$  kpc) from the photometric nucleus of the galaxy, which may be due to the peculiar development of the azimuthal  $m = 1$  harmonic in the gas velocity field (Emsellem, 2002). This asymmetric harmonic can be generated by the tidal interaction with the nearby companion NGC 474 studied by Turnbull et al. (1999). The observed displacement of the center can also be explained as resulting from the development of an asymmetric harmonic in the surface brightness distribution. As was pointed out by Zasov and Khoperskov (2002), this effect can be observed at certain evolutionary stages of barred galaxies.

The most peculiar galaxies (in terms of the gas kinematics) are NGC 3945 and NGC 5850. In the NGC 3945 the gas line-of-sight velocities within  $6''$  ( $0.5$  kpc) are close in maximum amplitude to the stellar velocities ( $80$  and  $120$   $\text{km s}^{-1}$ , respectively) but are opposite in sign! At large distances, the sense of rotation of the gas changes sharply and virtually coincides with that of the stars (Fig. 3h,i). The latter fact is also confirmed by the line-of-sight velocity measurements of the ionized gas with the IFP in several star-forming regions in the outer ring structure at distances  $120 - 140''$  ( $10 - 11$  kpc) from the center. It should be noted that such counter-rotation of the gas and stars is occasionally observed in early-type galaxies; it is commonly attributed to the absorption of an outer gas cloud (Bertola et al., 1992; Kuijken et al., 1996).

The dynamical axis of the stars in the circumnuclear region of NGC 5850 is close to the line of nodes, while in the ionized gas, this axis deviates from it by more than  $50 - 60^\circ$  (Fig. 5c) and is almost aligned with the position angle of the central isophotes. This behavior is typical of a disk inclined to the galactic plane (Moiseev and Mustsevo, 2000). In addition, if we, nevertheless, assume the gas motions to take place in the galactic plane, then it will turn out that they correspond to a radial outflow from the nucleus<sup>1</sup> with velocities  $50 - 70$   $\text{km s}^{-1}$ . Such features are characteristic of Seyfert galaxies, but the optical spectrum of the galaxy contains no emission lines indicative of an active nucleus, nor are starbursts observed here (Higdon et al., 1998). A more reasonable assumption is

<sup>1</sup> Here, we use the suggestion made by Higdon et al. (1998) that the disk orientation of the galaxy for which its western half is closest to the observer is most probable.

that the gas moves at  $r < 6 - 7''$  in a plane polar to the galactic disk. In this case, the polar gaseous disk lies almost exactly along the small cross section of the outer bar. In recent years, such polar minidisks associated with a large-scale bar or a triaxial bulge have been detected in the circumnuclear regions of several galaxies, for example, in NGC 2841 (Sil'chenko et al. 1997; Afanasiev and Sil'chenko, 1999) or NGC 4548 (Sil'chenko, 2002). The hypothesis of a polar disk is also supported by the fact that, according to Higdon et al., (1998), NGC 5850 has undergone a recent collision with the nearby galaxy NGC 5846. Through their interaction, part of the gas could be transported to polar orbits.

### 3.3. Minispirals

We used the HST archival images of the galaxies to study the detailed morphology of their circumnuclear regions. The models of mean elliptical isophotes were constructed by the standard technique and were subsequently subtracted from the original images. In five galaxies, the residual brightness distributions obtained in this way within their large-scale bars are in the shape of small spirals  $5 - 15''$  in size. A Fourier analysis of the azimuthal brightness distribution was used to quantitatively describe the detected spirals. The original images at each radius were expanded into the Fourier series (1), with the radius and the azimuthal angle in the galactic disk plane being applied for  $r$  and  $PA$ , respectively. The derived Fourier spectrum allows us to determine both the number of arms of the principal spiral harmonic and the location of the line of its maximum amplitude. Examples of spirals, their residual brightness, and the mean harmonic amplitudes in three galaxies are shown in Fig. 6.

Three of the minispirals studied have already been described in the literature: the pseudoring in NGC 2273 (Ferruit et al., 2000) and the flocculent spirals in NGC 4736 (Elmegreen et al., 2002) and in NGC 6951 (Pérez et al., 2000). Two new circumnuclear spirals were also found: the two-arm spiral in NGC 5566 and the three-arm spiral in NGC 7743. Based on an isophotal analysis of images, several authors (see references in the Table 1) pointed out the existence of a secondary inner bar in these galaxies. Within the bar, the line of maximum of the principal  $m = 2$  azimuthal harmonic must be elongated along the corresponding constant azimuth. In NGC 5566, however, this line is wound into a spiral that runs almost from the very center and coincides with the residual-brightness peak (Fig. 6b); i.e., a minispiral rather than a bar is located here, with its shape resembling the outlines of the spirals within the bars obtained in the model calculations by Englmaier and Shlosman (2000). The minispiral shown in Fig. 6b lies within a large scale bar with a semi-major axis of about  $30''$  ( $\sim 3$  kpc).

In NGC 3786, the line of maximum of the  $m = 2$  harmonic at  $r < 5 - 6''$  has a constant azimuthal angle, which is a further confirmation of the existence of a

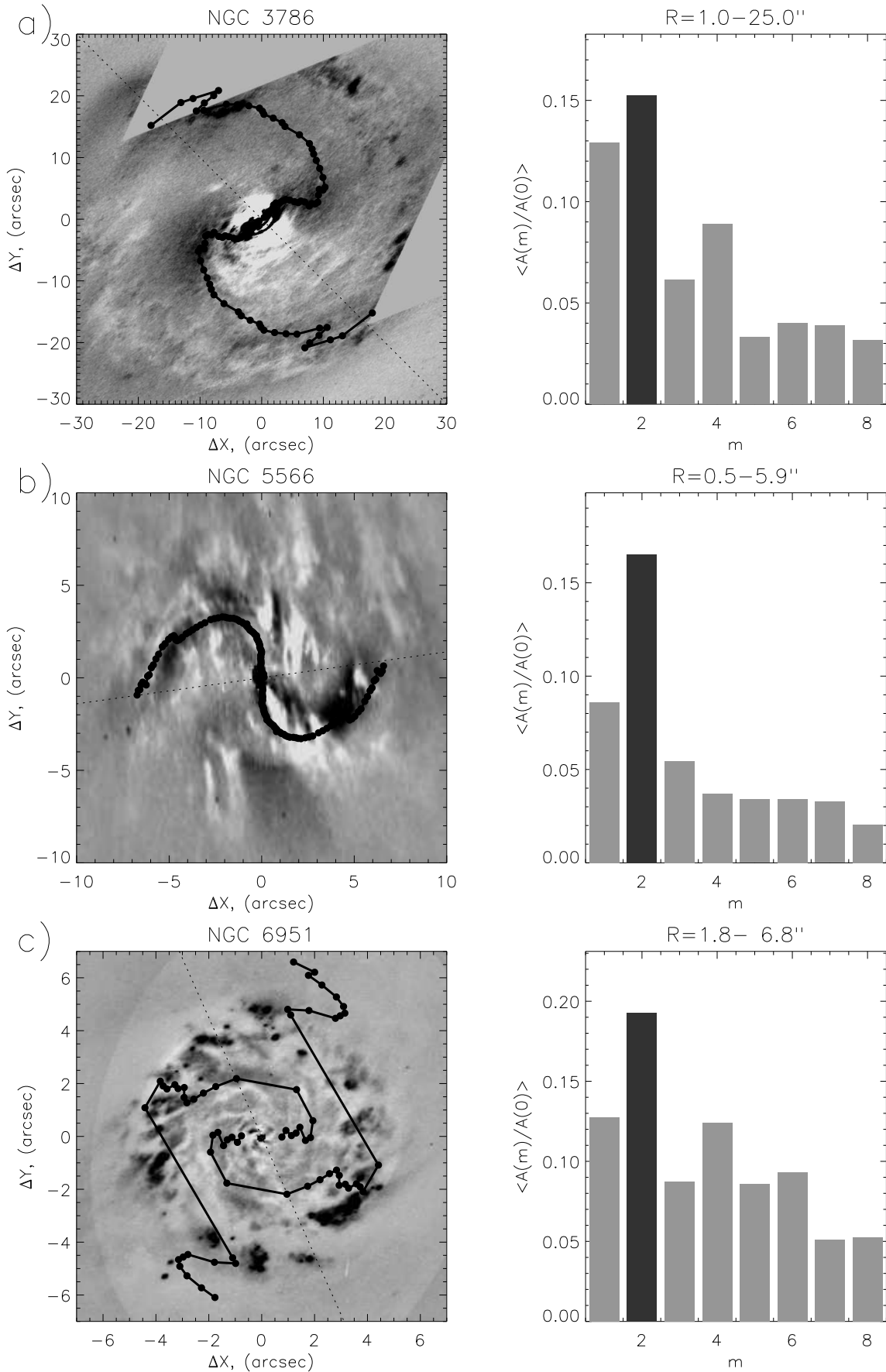


**Fig. 6.** The spiral patterns seen in the HST images (F606W filter): (a) NGC3786, (b) NGC5566, and (c) NGC6951. The maps of residual brightness in the galactic plane with the lines of maximum of the second harmonic in the brightness distribution superposed on them are shown on the left. The mean harmonic amplitude normalized to  $A_0$  is shown on the right; the range of radii ( $R = ..$ ) in which the averaging was performed is indicated.

minibar whose dynamical manifestations are described in Subsect. 3.2. Far from the center, this line is wound into a regular spiral that coincides with the global two-arm pattern in the galactic disk at  $r = 20 - 30''$ . The Fourier spectrum is dominated by the second harmonic; the  $m = 1$  harmonic is similar in amplitude to it (Fig. 6a). Clearly, the large relative amplitude of the first harmonic can be explained in terms of asymmetry in the apparent distribution of the dust lanes, most of which lie on the near side of the NGC 3786 disk. A similar effect was described by Fridman and Khoruzhii (2000) when performing a Fourier analysis of the images for NGC 157. The spirals, defined as the maximum of the  $m = 2$  harmonic near the bar ends, change their winding direction (Fig. 6a). According to Fridman and Khoruzhii (2000), this behavior must suggest that the bar is slow (in terms of the angular velocity of rigid rotation). For the nature of the minibar in NGC 3786 to be eventually elucidated, we must know a more detailed gas velocity field than that used here.

Wozniak et al. (1995) detected an isophotal twist at  $r < 5-6''$  in the ground-based optical images of NGC 6951 within its outer bar  $r \approx 60''$  in size, which they interpreted as an inner bar. However, based on near-infrared photometry, Friedli et al. (1996) questioned this interpretation by assuming that the isophotal twist could result from a complex distribution of dust and star-forming regions within the central kiloparsec. Indeed, the HST images exhibit a ring of star-forming regions that is elliptical in the plane of the sky but is almost circular in the galactic plane (the inclination of the galactic plane to the line of sight was assumed to be  $42^\circ$ , in agreement with the data of Pérez et al. (2000). These high-resolution images confirm the absence of a bar as an elongated, ellipsoidal structure. The  $m = 2$  harmonic dominates in the Fourier spectrum within the ring of star formation, but, in contrast to NGC 3786 and NGC 5566, the line of its maximum consists of separate fragments of the spirals. This is also true for higher harmonics, which, however, have a sufficiently high amplitude (Fig. 6c). If we draw an analogy with the classification of large-scale spiral arms, then a grand design is observed in NGC 3786 and NGC 5566 and flocculent spirals are observed in NGC 6951 and NGC 4736. However, the minispiral in NGC 6951 differs from the large-scale spirals in disk galaxies in that the multi-arm spiral seen in the residual-intensity distribution (Fig. 6c) is probably associated only with the distribution of gas and dust rather than with the stellar component. As was shown by Pérez et al. (2000), this inner spiral structure clearly seen in the V band completely disappears in the H band, where the effect of dust absorption is much weaker.

Interestingly, the position angle of the dynamical axis constructed from the ionized-gas velocity field in the  $H_\alpha$  and  $[N II]$  lines at  $r = 0 - 8''$  deviates by  $10 - 15^\circ$  from the line of nodes of the outer disk, suggesting a significant role of non-circular motions. Since there is no inner bar here, we can offer the following interpretation of the observed pattern. There is a gas-and-dust disk  $6 - 8''$  ( $400 - 600$  pc) in radius within the large-scale bar in which

a multiarmed spiral structure perturbing the circumnuclear gas rotation develops. The dynamical decoupling of this disk is also confirmed by a high molecular-gas density (Kohno et al. 1999) and by the location of two inner Lindblad resonances of the large-scale bar here<sup>2</sup> (Pérez et al., 2000).

Presently, minispirals have been detected in the circumnuclear regions of many galaxies (Carollo et al., 1998), but as yet no unequivocal interpretation of the nature of their formation has been offered [see Elmegreen et al., (2002) for more details]. One of the reasons why the theoretical interpretations have failed seems to be the scarcity of reliable data on the observed kinematics of such spirals. The papers on this subject are still few in number (Laine et al., 2001; Schinnerer et al., 2002) and from this point of view, measurements of the gas velocities at the center of NGC 6951 can be of interest in their own right.

#### 4. Discussion

The main motive for this study is the search for any common features in the kinematics of bar-within-bar structures in an attempt to prove that the secondary bar is dynamically decoupled. A similar attempt has recently been also made by Emsellem et al. (2001), who presented the results of their study of stellar motions in four southern-sky galaxies. Using the method of “classical” long-slit spectroscopy Emsellem et al., (2001) concluded that the inner bars were decoupled in three objects based only on the existence of a circumnuclear line-of-sight velocity peak in long-slit cuts. However, such features can also be explained in terms of more natural factors, such as a peculiar mass distribution in the disk and the bulge or non-circular motions in the outer bar, without invoking the hypothesis of a secondary bar. Observations of two-dimensional kinematics, which allow the pattern of non-circular gas and stellar motions to be determined, could give a more definitive answer. The results obtained in this way appear all the more unexpected.

First, the shape of the line-of-sight stellar velocity dispersion distribution (Subsect. 3.1) is determined only by the outer bar and does not depend on the relative position of the inner bar-like structure. Second, either non-circular motions typical of the outer bar or good agreement with circular rotation are observed in the stellar velocity fields; the latter is, probably, explained by the fact that here, the line-of-sight stellar motions in the bar and the bulge are added together (Subsect. 3.2). Finally, the ionized-gas velocity fields everywhere point to the presence of noticeable non-circular motions. However, they either correspond to the outer bar (as suggested by from analysis of the radial behavior of  $PA_{dym}$ ) or are associated with the inner spiral structure (NGC 6951) or with another individual

<sup>2</sup> When the paper was submitted for publication, the paper by Rozas et al., (2002) appeared. Based on their IFP observations, these authors reached a similar conclusion regarding the nature of the inner disk in NGC 6951.

peculiar features of the galaxy (NGC 470, NGC 3945, and NGC 5850). Thus, it turns out that the secondary inner bar seen in the galaxy images does not affect the observed kinematics of the gas and stellar components in all the sample objects.

This conclusion is in conflict with the popular opinion of a dynamically independent secondary bar, which is based on analysis of isophotal shapes and on model calculations (Sect. 1). Maybe the methods used here and the limited spatial resolution do not allow the kinematic features of the small-scale inner bar to be evaluated. However, this is not the case, because the minibars in NGC 3368 and NGC 3786 do not differ in their apparent sizes from the secondary bars in the remaining galaxies (see the Table 1), but the features of non-circular gas and stellar motions associated with them are clearly detected. In this case, our photometric analysis suggests that there is no outer bar in these two galaxies (Subsects. 3.2 and 3.3).

The three galaxies with the most peculiar features in the observed gas motions should be considered separately. Although the asymmetric  $m = 1$  mode developed within the bar of NGC 470 and the polar gaseous disk in NGC 5850 are rare structures, they, nevertheless, were observed by several authors in other objects as well (see Subsect. 3.2). It was also noted in this subsection that the two galaxies have close massive companions. Therefore, the assumption that the features of their gas kinematics result from the interaction with the companions appears reasonable enough.

According to Kuijken et al., (1996), the gaseous disks in lenticular (S0) galaxies exhibit counter-rotation relative to the stars in  $24 \pm 8\%$  of the cases<sup>3</sup>; i. e. , this is a common phenomenon that is, probably, attributable to merging of the fallen gaseous cloud with the corresponding direction of angular momentum (Bertola et al., 1992). Against this background, the gas counter-rotation at the center of NGC 3945, one of the four S0 galaxies in our sample (table 1) with gaseous disks observed in three of them (NGC 2681, NGC 3945, and NGC 7743), comes as no surprise.

The presence of minispirals in some galaxies is not surprising either. Thus, Erwin and Sparke (2002) found that their sample of early-type (S0-Sa) barred galaxies contained  $24 \pm 7\%$  of objects with circumnuclear minispirals, which is slightly less than  $39 \pm 14\%$  (5 of 13) in the sample under study. Although the difference between the frequencies of occurrence of minispirals is within the error limits, it can be easily explained in terms of the selection effect in the sample of galaxies with inner isophotal twists. The inner spirals distort the central isophotes, which may lead to the wrong conclusion that there is a secondary bar.

Having studied the detailed kinematics of the gas and stars in the galaxies from our sample, we may conclude that the so-called double-barred galaxies are not a separate type of galaxies but are a combination of objects

with distinctly different structures of their circumnuclear regions. The formal use of isophotal analysis of images to study galaxies without invoking kinematic data can lead to erroneous conclusions. We think that the double-barred galaxies described in the literature can be arbitrarily divided into two basic classes. The first class includes early-type (S0-Sa) galaxies. Here, the illusion of a secondary bar results from the triaxial bulge shape. In contrast to the bar, the triaxial bulge has virtually no effect on the disk dynamics in the circumnuclear region. A characteristic example is NGC 2950. The second class includes galaxies of later types. Here, decoupled gas-and-dust disks with a minispiral structure distorting the isophotal shape can be observed within large-scale bars. A characteristic example is NGC 6951. There is also a third possibility. The  $x_2$  family of stable orbits oriented perpendicular to the bar major axis can exist within a large-scale bar (Contopoulos and Grosbøl, 1989). A bar-like structure that is exactly perpendicular to the primary bar and that correspondingly distorts the observed isophotes can be formed on the basis of these orbits. Such a model was proposed for NGC 2273 (Petitpas and Wilson, 2002). In this case, however, there is no decoupled secondary bar but there is a feature in the inner structure of the major bar that rotates with it as a whole.

## 5. Conclusions

A number of contradictions between existing models of nested bars and observations can be resolved by abandoning the popular view of dynamically independent double bars, which we propose here. Many models suggest that the secondary bar is a short-lived structure, which, in turn, is in conflict with common observations of inner isophotal twists [see Erwin and Sparke (2002) for more details]. However, all falls into place if these twists are not associated with the secondary bars, at least in most of these galaxies. On the other hand, the fact that, according to statistical data, the photometric secondary bar is in no way associated with the presence of an active nucleus in the galaxy can be explained (Laine et al., 2002; Erwin and Sparke, 2002), although it is clear from theoretical considerations that the correlation here must be much closer than that for single bars. The reason is that the secondary bar traceable by isophotal twists is not a dynamically decoupled structure in the galaxy at all.

*Acknowledgements.* I wish to thank V.L. Afanasiev for interest and helpful discussions and N.V. Orlova for help in preparing the article. This study is based on observational data obtained with the 6m Special Astrophysical Observatory telescope financed by the Ministry of Science of Russia (registration no. 01-43) and on HST NASA/ESA data taken from the archive of the Space Science Telescope Institute operated by the Association of Universities for Research in Astronomy under a contract with NASA (NAS 5-26555). In my work, I used the NASA/IPAC (NED) Extragalactic Database operated by the Jet Propulsion Laboratory of the California Institute of Technology under a contact with the

<sup>3</sup> In what follows, the errors are given at a  $1\sigma$  level of the binomial distribution.

National Aeronautics and Space Administration (USA) and the HYPERCAT database (France). The study was supported by the Russian Foundation for Basic Research (project nos. 01-02-17597 and 02-02-06048mas) and the Federal Program “Astronomy” (project no. 1.2.3.1).

## References

- Afanasiev V.L. & Shapovalova A.I., 1981, *Astrophysics*, 17, 221  
 Afanasiev V.L. & Sil’chenko O.K., 1999, *AJ*, 117, 1725  
 Afanasiev V.L., Mikhailov V.P., Shapovalova A.I., 1998, *Astron. Astrophys. Trans*, 16, 257  
 Afanasiev V.L., Dodonov S.N., Moiseev A.V., 2001, *Stellar dynamics: from classic to modern*, eds. Osipkov L.P., Nikiforov I.I., Saint Petersburg, 103  
 Begeman K.G., 1989, *A&A*, 223, 47  
 Bertola F., Buson L.M., Zeilinger W.W., 1992, *ApJ*, 401, L79  
 Buta R., Crocker D.A., 1993, *AJ*, 105, 1344  
 Carollo C.M., Stiavelli M., Mack J., 1998, *AJ*, 116, 68  
 Chevalier R.A., & Furenid I., 1978, *AJ*, 225, 67  
 Combes F., 2001, in *Advanced Lectures on the Starburst- AGN Connection*, Ed. by I. Aretxaga, D. Kunth, & R. Mejica (World Scientific, Singapore, 2001), 223, (astro-ph/0010570)  
 Contopoulos G., & Grosbol P., 1989, *A&A Rev.*, 1, 261  
 de Vaucouleurs G., 1975, *ApJs*, 29, 193  
 Duval M.F., & Monnet G., 1985, *A&AS*, 61, 141  
 Elmegreen D.M., Elmegreen B.G., Eberwein K.S, 2002, *ApJ*, 564, 234  
 Emsellem E., 2002, (astro-ph/0202522)  
 Emsellem E., Greusard D., Combes F., et al., *A&A*, 2001, 368, 52  
 Englmaier P., & Shlosman I., 2000, *ApJ*, 528, 677  
 Erwin P., & Sparke L.S., 1999, *ApJ*, 521, L37  
 Erwin P., & Sparke L.S., 2002, *AJ*, 124, 65  
 Ferruit P., Wilson A. S., Mulchaey J., 2000, *ApJs*, 128, 139  
 Frei Z., Guhathakurta P., Gunn J.E., Tyson J.A., 1996, *AJ*, 111, 174  
 Fridman A.M., & Khoruzhii O.V., 2000, *Phys. Lett. A*, 276, 199  
 Fridman A. M., Khoruzhii O. V., Polyachenko E. V., et al., 2001b, *MNRAS*, 323, 651  
 Friedli D., & Martinet L., 1993, *A&A*, 277, 27  
 Friedli D., Wozniak H., Rieke M., Martinet L., Bratschi P., 1996, *A&AS*, 118, 461  
 Heller C., Shlosman I., Englmaier P., 2001, *ApJ*, 553, 661  
 Higdon J., Buta R., Purcel G.B., 1998, *AJ*, 115, 80  
 Jungwiert B., Combes F., Axon D.J., 1997, *A&AS*, 125, 479  
 Khoperskov A.V., Zasov A.V., Tyurina N.V., 2002, *Astron. Reports*, 45, 180  
 Khoperskov A.V., Moiseev A.V., Chulanova E.A., 2001, *Bull. Spec. Astrophys. Obs.*, 52, 135  
 Knapen J.H., Shlosman I., Heller C.H., et al., 2000a, *ApJ*, 528, 219  
 Knapen J.H., Shlosman I., Peletier R.F, 2002b, *ApJ*, 529, 93  
 Kohno K., Kawabe R., Vila-Vilaro B., 1999, *ApJ*, 511, 157  
 Kormendy J., 1982, *ApJ*, 257, 75  
 Kormendy J., 1983, *ApJ*, 275, 529  
 Kuijken K., Fisher D., Merrifield M.R., 1996, *MNRAS*, 283, 543  
 Laine S., Knapen J.H., Pérez-Ramírez D., et al., 2001, *MNRAS*, 324, 891  
 Laine, S., Shlosman, I., Knapen, J.H., Peletier R.F., 2002, *ApJ*, 567, 97  
 Lindblad P.O., 1999, *A&A Rev.* 9, 221  
 Lyakhovich V.V., Fridman A.M., Khoruzhii O.V., Pavlov A.I., 1997, *Astron. Reports*, 41, 447  
 Maciejewski W., Sparke L.S., 2000, *MNRAS*, 313 745  
 W. Maciejewski, J. Teuben, L. S. Sparke, & J. M. Stone, *Mon. Not. R. Astron. Soc.* 329, 502 (2002).  
 Maciejewski W., Teuben J., Sparke L.S., Stone J.M., 2002, *MNRAS*, 329 502  
 Moiseev A.V., 2001a, *Bull. Spec. Astrophys. Obs.*, 51, 11 (astro-ph/0111219)  
 Moiseev A.V., 2001b, *Bull. Spec. Astrophys. Obs.*, 51, 11 (astro-ph/0111219)  
 Moiseev A.V., 2002, *Bull. Spec. Astrophys. Obs.*, 54, (astro-ph/0211104)  
 Moiseev, A.V., & Mustsevoi V.V, 2000, *Astro. Letter.*, 26, 665 (astro-ph/0011225)  
 Moiseev, A.V., Valdes, J.R., Chavushan, V.O., 2002, Preprint SAO RAS, No. 171, submitted to *A&A*  
 Monnet G., Bacon R., Emsellem E., 1992, *A&A*, 253, 366  
 Mulchaey J.S., Regan M.W., Kundu A., 1997, *ApJs*, 110, 299  
 Pérez E., Márquez I., Durret F., et al., 2000, *A&A*, 353, 893  
 Petitpas G.R., & Wilson C.D., 2002, *ApJ*, 575, 814  
 Pfenninger, D., & Norman, C.A., 1990, *ApJ*, 363, 391  
 Rozas M., Relano M., Zurita A., Beckman J. E., 2002, *A&A*, 386 42  
 Sakamoto K., Okumura S.K., Ishizuki S., Scoville N.Z., 1999, *ApJ*, 525, 691  
 Schinnerer E., W. Maciejewski W., Scoville N., Moustakas L.A., 2002, *ApJ*, 575, 826  
 Selwood J.A., & Wilkinson A., 1993, *Rep. Prog. Phys.* 56, 173  
 Shaw M.A., Combes F., Axon D.J., Wright G.S., 1993, *A&A*, 273, 31  
 Shlosman I., Frank J., Begeman M.C., 1989, *Nature*, 338, 45  
 Shlosman I., & Heller C., 2002, *ApJ*, 565, 921  
 Sil’chenko O.K., Burenkov A.N., & Vlasyuk V.V., 1997, *A&A*, 326, 941  
 Sil’chenko O.K., 2002, *Astron. Lett.*, 28, 207  
 Sil’chenko, O.K., Moiseev, A.V., Afanasiev, V.L., Valdés J.R., Chavushan V.O., 2003, submitted to *AJ*  
 Turnbull, A.J., Bridges, A.J., Carter, D., 1997, *MNRAS*, 307, 967  
 Vauterin P., & Dejonghe H., 1997, *MNRAS*, 286, 812  
 Wozniak H., Friedli D., Martinet L., Martin P., Bratschi P., 1995, *A&AS*, 111, 115  
 Zasov, A.V. & Khoperskov, A.V., 2002, *Astronomy Reports*, 46, 173

*Translated by V. Astakhov*